ISBN: 978-3-95450-262-2 ISSN: 2673-5350 doi: 10.18429/JACoW-IBIC2025-TUPMO35

IMPROVED DESIGN OF THE EMITTANCEMETER FOR THE C-BAND PHOTOINJECTOR AT IHEP*

W. Chen[1,2], F. Li[1,2], R. Yang†[,1,2], B. Zhang[1,2]
[1]Institute of High Energy Physics, Beijing, China
[2]China Spallation Neutron Source, Dongguan, China

Abstract

To enhance the performance of next-generation X-ray Free Electron Lasers (XFELs), the high-quality driven beam with a low emittance, particularly for attaining emittances below 0.2 mm·mrad for 100 pC bunch charges, is of great importance. The use of a C-band photocathode RF gun is one of the promising routines to deliver such low-emittance beam. Prior to the commissioning of beams from such an injector, a precise and efficient measurement tool must be established. In this report, we introduce an emittance measurement method using an orthogonal dual-slit technique, aimed at enhancing measurement efficiency and achieving the necessary measurement accuracy for such small emittances. The primary parameters, for instance, the slit width, the beamlet drift distance, the sub-beamlet drift distance, are optimized through numerical simulations.

INTRODUCTION

The X-ray free electron laser driven by high-brightness electron beams is a cutting-edge tool for studying atoms and molecules with unprecedented temporal and spatial resolutions. Most current XFELs operate with normalized transverse emittances below 1 mm·mrad [1]. To make XFELs more affordable and accessible, compact designs with lower linac energies have been proposed [2], which requires an high-brightness electron source [3, 4].

Among the feasible high-bright electron sources, the high-gradient RF gun with a low-intrinsic-emittance photocathode is promising. For photocathode RF guns, emittance minimizes at gradients about 140-150 MV/m [5, 6]. However, the L-band and S-band RF guns can only reach a stable acceleration gradient of about 120 MV/m [7, 8].To achieve a higher acceleration gradient, the RF gun operating at an elevated resonant frequency like C-band or X-band has been developed in recent years [9–11]. Among them, the C-band photocathode RF gun features a maximum gradient about 150 MV/m and can provide a normalized emittance of below 0.2 mm·mrad with a bunch charge of 100 pC.

As a starting element of linear injector for the future Southern Advanced Light Source (SAPS), a C-band photoinjector test platform has been proposed and is under construction at Institute of High Energy Physics (IHEP). This test platform employs a 3.6-cell normal conducting RF gun operating at 5.712 GHz. With a designed acceleration gradient of about 150 MV/m, the expected normalized emittance is lower than 0.2 mm·mrad for a bunch charge of 100 pC [12]. The primary parameters are summarized in Table. 1. Towards the successful commissioning and operation of this C-band RF gun, a short diagnostic beamline has been designed. It consists of an emittancemeter (EM), an integrating current transformer (ICT), an energy measuring instrument consisting of two slits and a screen, and a Faraday cup (FC), as shown in Fig. 1.

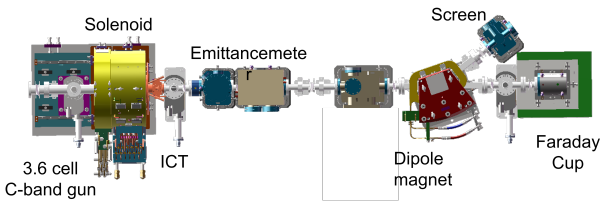

Figure 1: Schematic diagram of the C-band photocathode RF gun test platform at IHEP.

Table 1: The Major Beam Parameters at the Gun Exit for a Bunch Charge of 100 pC

Parameter	Unit	Value
RF frequency	GHz	5.712
Accelerating gradient	MV/m	150
Beam energy	MeV	7.3
95 % emittance	mm·mrad	0.11
RMS beam size	μm	42.5
RMS beam divergence	mrad	0.37
RMS bunch length	ps	5

In the previous studies, a new emittance diagnostic scheme based upon parallel-slit scan was proposed and optimized [13, 14]. To further improve the accuracy of the emittance measurement at the exit of the RF gun, an orthogonal-slit scan scheme has been recently proposed and evaluated through numerical simulations. For a target 95 % emittance of 0.1–0.2 mm·mrad, a measurement error of 5–10 % is achieved employing this orthogonal-slit scan method.

FROM PARALLEL-SLIT SCAN TO ORTHOGONAL-SLIT SCAN

The parallel dual-slit scan method operates on the similar principle as the single-slit method, but offers a key advantage: it significantly reduces space charge effects, leading to higher measurement precision, with a measurement error less than 10 % for measuring 100 pC beam emittance

* Work supported by National Natural Science Foundation of China (No. 12305166) and the Natural Science Foundation of Guangdong Province, China (No. 2024A1515010016).
† yangrenjun@ihep.ac.cn

ISBN: 978-3-95450-262-2 ISSN: 2673-5350 doi: 10.18429/JACoW-IBIC2025-TUPMO35

below 0.2 mm·mrad [13, 14]. However, the need for precise alignment of the two slits adds further hardware complexity and measures emittance in only one direction. In order to enhance the diagnostic efficiency with acceptable measurement accuracy, a method employing an orthogonal dual-slit scan is therefore proposed and optimized through the PIC simulations. This approach retains the fabrication advantages of slit masks while enabling efficient reconstruction of the complete 4D phase space. It employs two slits of identical width. The first slit is scanned across the beam in one transverse direction (e.g., horizontal), and at each position, the second, orthogonally-oriented slit is scanned in the perpendicular direction (e.g., vertical). After performing N horizontal and M vertical scans (i.e., $N \times M$ measurements), the full 4D transverse phase space distribution can be reconstructed. Compared to the pepper-pot method, our technique offers two key advantages: it simplifies the mechanical fabrication challenge and provides a more flexible and accurate approach to complete phase-space characterization.

A schematic of the orthogonal dual-slit setup is depicted in Fig. 2. The first slit divides the beam into a series of horizontal beamlets with reduced charges, lowering the charge density and thus decreasing space charge forces in the horizontal direction. The second slit in vertical direction, positioned at a distance L_1 downstream, further reduces the beamlet's vertical dimension, mitigating space charge forces in both horizontal and vertical directions. After the horizontal first slit, the resulting sub-beamlet reflects the angle distribution at a fixed horizontal position in phase space. Following the vertical second slit cutting, the sub-beamlet represents a intensity-sliced angular distribution in the horizontal phase space.

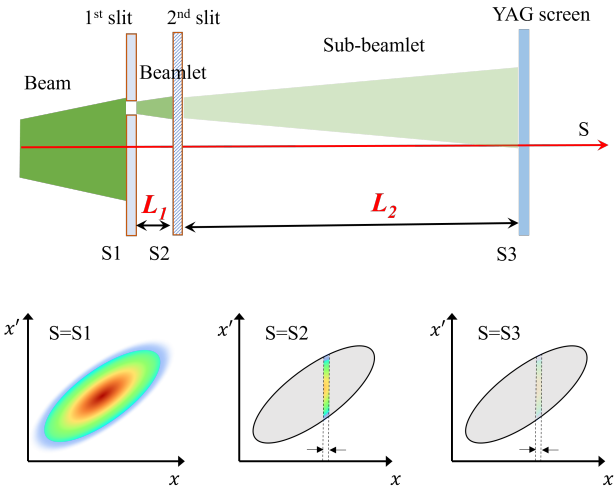

Figure 2: A schematic layout of the emittance measurement device based on orthogonal dual-slit scheme.

Estimations of the Space-Charge Field

To evaluate the space charge field of the beamlet and sub-beamlet, a Python script has been prepared. It uses a symplectic self-consistent space-charge model with a gridless spectral method to calculate space-charge [15, 16].

Both the single-slit and orthogonal dual-slit methods generate beamlets by cutting the initial beam, allowing a focused comparison of space charge effects under different cutting scenarios: no further division versus additional slit. Compared to the initial beamlet, the peak field strength of the space charge force along the vertical direction on the sub-beamlet is reduced by 61 % after a horizontal slit and by 73 % after a vertical slit, as shown in Fig. 3.

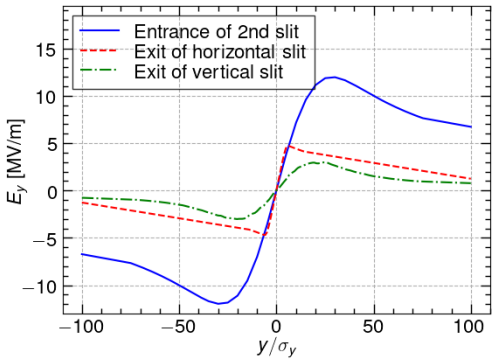

Figure 3: The assessed space-charge field for a beamlet and subsequent sub-beamlets.

PERFORMANCE OF THE ORTHOGONAL-SLIT SCAN SCHEME

To achieve the precision (< 10 %) required for measuring small emittance of the C-band RF gun's beam, dynamic errors in the linear actuator and imaging system must be minimized. The primary sources of measurement inaccuracy are the displacement precision of the linear actuator, which affects the scanning of the slit, and the imaging resolution of the beamlet profile monitor, which impacts beamlet size measurement. Poor displacement accuracy may cause overlapping or missing beam slices, hindering accurate phase-space reconstruction, while insufficient imaging resolution distorts the beamlet profile. To evaluate the method's accuracy, we first assess hardware errors (actuator and imaging), then optimize the design through PIC simulations.

The positional accuracy of the linear actuators has been calibrated using an extra laser tracker (Leica AT901) [17]. The displacement accuracy of the two linear actuators are approximately 0.6 µm and 0.9 µm over 10 µm steps, as depicted in Fig. 4.

For the chosen zoom lens (TS-93022), the spatial resolution of the cameras can be determined by the imaging experiment of the USAF1951 resolution test chart. In the experiments, a CMOS camera (Balser 4200gm) and a sCMOS camera (pco.edge 5.5 RS) have been employed as image sensors. For a magnification of 3, a spatial resolution of better than 7 µm has been measured. As a conservative estimation, a spatial resolution of better than 10 µm is assumed for the later simulations.

ISBN: 978-3-95450-262-2 ISSN: 2673-5350 doi: 10.18429/JACoW-IBIC2025-TUPMO35

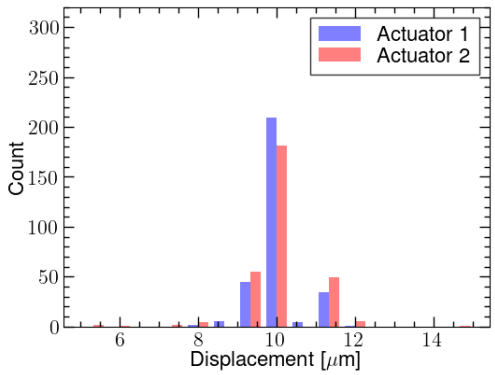

Figure 4: Positional accuracy of two linear actuators with grating ruler feedback, measured using a laser tracker.

Optimizations of the Emittancemeter

We have used the ASTRA particle tracing program [18] and a Python script to optimize the slit structure. ASTRA traces particles with 2.5×10^5 macro-particles using 3D FFT, while Python handles slit screening with a 4D linear transfer matrix. When a particle's coordinates exceed the slit acceptance, the particle loss at the slit mask without creating any secondary particles. The actuator's position error (10 µm) was simulated to account and the spatial resolution (10 µm) of the optical observation system was modeled.

Notice that the measurement accuracy depends on the algorithm used for emittance analysis. Due to a limited signal-to-noise ratio (SNR), imperfect image noise subtraction, and weak signal recognition, it is impossible to reconstruct 100 % of the emittance. Instead, henceforth, the 95 % emittance, encompassing 95 % of the bunch charge, is calculated using the threshold method [19, 20].

Theoretically the influence of the space charge force on the emittance measurement can be minimized when the gap between the two slits is zero. However, due to the actual hardware volume limitations, as well as considering the stability of the motor, a small gap between the two slits should be recommended. For simplicity, L_1 is set to 1 mm in the simulations. Moreover, a slit mask with a thickness of 1 mm is considered following the previous design studies.

Similarly, the orthogonal dual-slit scanning method needs to optimize the L_2 concering the above dynamic errors. For a 100 pC beam with emittance of 0.18 mm·mrad, 42.5 µm RMS beam size, using orthogonal dual-slits with $L_1 = 2$ mm and $L_2 > 0.2$ m, emittance measurement errors are below 4.9 % for slit widths of 10 µm. Extending this to a narrower slit width of 8 µm, using orthogonal dual-slits with $L_1 = 2$ mm and $L_2 > 0.2$ m, the emittance measurement errors remain below 1.9 % for the 8 µm slit width. Narrower slits (e.g., 5 µm) can reduce errors to approximately −3 %, but increasing beam loss at the slit walls, leading to incomplete phase-space reconstruction for a 100 pC bunch, as shown in Fig. 5. The particle loss causing by slit acceptance is 10.6 %, 7.3 %, 6.7 %, for 5 µm, 8 µm, and 10 µm, respectively. To mitigate beam loss while maintaining low errors, a slit width of 10 µm is recommended, balancing a 6 % measurement error.

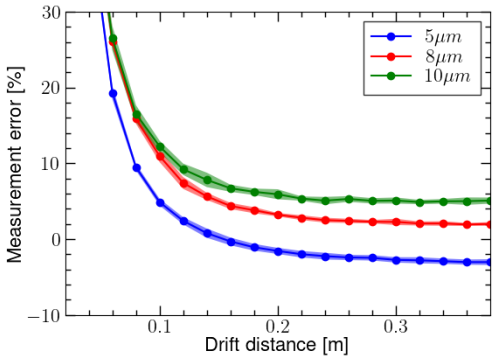

Figure 5: Emittance measurement error as a function of the sub-beamlet drift distance for a bunch charge of 100 pC.

Using orthogonal slits, where the vertical slit scans the beam to form a w µm × w µm square micro-hole with the horizontal slit, the horizontal beamlet distribution reconstructs the beam's horizontal phase space and emittance. Similarly, scanning with the horizontal slit as a reference yields the vertical phase space and emittance. Regarding the beam parameters of a C-band photocathode RF gun, a 10 µm slit width is a optimal balance of accuracy and beam loss.

CONCLUSION

This paper addresses the critical need to accurately measure emittance from a C-band photocathode RF gun. To achieve this, we have proposed an orthogonal-slit scan method. In the design process, dynamic errors, slit scanning accuracy and downstream profile detection resolution, were quantified through theoretical analysis and experimental measurements. With the optimized drift distances, an emittance measurement error of less than 10 % has been indicated, employing two slits with a 10 µm width and 1 mm depth. In the future, experimental demonstrations are proposed to validate these analytical evaluations.

REFERENCES

[1] H. Qian *et al.*, "Analysis of photoinjector transverse phase space in action and phase coordinates", *Phys. Rev. Accel. Beams*, vol. 25, p. 103401, 2022. doi:10.1103/PhysRevAccelBeams.25.103401

[2] J. B. Rosenzweig *et al.*, "An ultra-compact X-ray free-electron laser", *New J. Phys.*, vol. 22, no. 9, p. 093067, Sep. 2020. doi:10.1088/1367-2630/abb16c

[3] T. O. Raubenheimer, "The LCLS-II-HE, a high energy upgrade of the LCLS-II", in *Proc. FLS'18*, Shanghai, China, Mar. 2018, pp. 6–11. doi:10.18429/JACoW-FLS2018-MOP1WA02

[4] G. D'Auria *et al.*, "The CompactLight design study", *Eur. Phys. J. Spec. Top.*, vol. 233, pp. 1–208, 2024. doi:10.1140/epjs/s11734-023-01076-0

ISBN: 978-3-95450-262-2 ISSN: 2673-5350 doi: 10.18429/JACoW-IBIC2025-TUPMO35

[5] D. Palmer *et al.*, "Initial commissioning results of the next generation photoinjector", *ASCE*, pp. 695–704, 1997.

[6] B. Dwersteg *et al.*, "RF gun design for the TESLA VUV free electron laser", *Nucl. Instrum. Methods Phys. Res. A.*, vol. 393, pp. 93–95, 1997. doi:10.1016/S0168-9002(97)00434-8

[7] L. Zheng *et al.*, "Development of S-band photocathode RF guns at Tsinghua University", *Nucl. Instrum. Methods Phys. Res. A.*, vol. 834, p. 98, 2016. doi:10.1016/j.nima.2016.07.015

[8] H. Xu *et al.*, "Development of an L-band photocathode RF gun at Tsinghua University", *Nucl. Instrum. Methods Phys. Res. A.*, vol. 985, p. 164675, 2021. doi:10.1016/j.nima.2020.164675

[9] C. Wang *et al.*, "Design optimization and cold RF test of a 2.6-cell cryogenic RF gun", *Nucl. Sci. Tech.*, vol. 32, no. 9, p. 97, 2021. doi:10.1007/s41365-021-00925-8

[10] L. Wang *et al.*, "Design, fabrication and cold-test results of a 3.6 cell C-band photocathode RF gun for SXFEL", *Nucl. Instrum. Methods Phys. Res. A.*, vol. 1003, p. 165320, 2021. doi:10.1016/j.nima.2021.165320

[11] A. Giribono *et al.*, "Dynamics studies of high brightness electron beams in a normal conducting, high repetition rate C-band injector", *Phys. Rev. Accel. Beams*, vol. 26, no. 8, p. 083402, 2023. doi:10.1103/PhysRevAccelBeams.26.083402

[12] X. Liu *et al.*, "A C-band test platform for the development of RF photocathode and high gradient accelerating structures", *J. Phys.: Conf. Ser.*, vol. 2687, p. 042001, 2024. doi:10.1088/1742-6596/2687/4/042001

[13] R. Yang *et al.*, "A consecutive double-slit emittance meter for high-brightness electron source", in *Proc. IPAC'23*, Venice, Italy, May 2023, pp. 4721–4724. doi:10.18429/JACoW-IPAC2023-THPL110

[14] W. Chen *et al.*, "Optimized design of an consecutive double-slit emittancemeter for the c-band photocathode rf gun", in *Proc. IBIC'24*, Beijing, China, Sep. 2024, pp. 266–270. doi:10.18429/JACoW-IBIC2024-WEP10

[15] J. Qiang, "Symplectic multiparticle tracking model for self-consistent space-charge simulation", *Phys. Rev. Accel. Beams*, vol. 20, no. 1, p. 014203, Jan. 2017. doi:10.1103/PhysRevAccelBeams.20.014203

[16] Sctracker repository, `https://gitlab.desy.de/xiangkun.li/sctracker`

[17] *AbsoluteTracker*, Leica Geosystems AG. `https://support.hexagonmi.com/s/article/AT901-Absolute-Tracker-User-Manual-v2-0-1en-1528376809911`

[18] ASTRA, `https://www.desy.de/~mpyflo/`

[19] M. Krasilnikov *et al.*, "Experimentally minimized beam emittance from an L-band photoinjector", *Phys. Rev. Spec. Top. Accel. Beams*, vol. 15, p. 100701, Oct. 2012. doi:10.1103/PhysRevSTAB.15.100701

[20] V. Miltchev, "Modelling the transverse phase space and core emittance studies at PITZ", in *Proc. FEL'05*, Palo Alto, California, USA, Aug. 2005, paper THPP041. `https://jacow.org/f05/papers/THPP041.pdf`